

Use of Natural Material – Clay for Sustainable Treatment of Water Polluted By Dyes

Soniya Sharma¹, Dr. Geetha Sarasan²

^{1,2}Department of Chemistry, Govt. Holkar Science College, Indore-452001, M.P., India

Abstract: Apart from the colorful side of dyes, the harmful effects they impose on environment cannot be overlooked. Treatment of water containing these dye effluents is today's demand. For encouraging methods that are sustainable for the desired purpose, use of natural materials like clay is suggested. Clay treated with acid called as acid activated clay (AAC) are efficient adsorbents when adsorption is chosen among other methods. Characterization of AAC was done using EDX, XRD, FTIR and SEM. Specific surface area and pore size determinations were also done. To test the efficiency of AAC for removal of BV2 dye from aqueous solution was done by varying different parameters. It was found that % removal increased from 78.77 % to 98.14 % for increasing dye concentration. Best adsorbent dose was found to be 0.05 gm. Alkaline pH favors the adsorption of basic dye. Rate of adsorption was in good correlation with pseudo second order kinetics. Adsorption mechanism was governed by surface diffusion as predicted from IPD and Boyd kinetic models. Surface morphological studies using SEM and FTIR shows changes in surface of adsorbent after adsorption. From the present study, it is suggested that acid activated clay can be effectively used as adsorbent for sustainable development of society.

Keywords: acid activated clay, adsorption, adsorption capacity, dyes, sustainable.

Date of Submission: 14-09-2017

Date of acceptance: 21-09-2017

I. Introduction

For the development of sustainable society, use of natural materials has been encouraged in every walk of life. Industrial techniques have to be modified using green route, to reduce toxic chemicals and their harmful impacts on environment [1]. Water is precious though it is available in plenty on earth but only 1% of it is useful to us. It is getting polluted due to growing industrialization to meet the increasing demands of boosting population [2]. Water pollution actually becomes a serious issue when dye effluents from textile and other industries get mixed with fresh water. These synthetic dyes persist in water as they are stable in light, resist biological treatment process and acts as oxidizing agents[3]. Various water treatment methods like chemical[4], biological[5], electrochemical[6] and others have been used for the removal of dyes from waste water. These methods do not completely remove dyes from water and their breakdown products remain in it causing toxicity to life. Among all the available methods, adsorption is one of the most effective physical method and is strongly favored as it is simple, economically feasible, easy to operate and sludge formation is minimum[2], [7].

For sustainable treatment process, adsorption using natural material like clay can be preferred as they are abundant, readily available, cheap and have good efficiency as adsorbent[3]. Efficiency of clay in dye removal can be enhanced by activating it. Acid activation is easiest method to improve the surface area, porosity, surface acidity and adsorption capacity of clay[8]. Thus Acid activated clay are attractive alternative to treat water having dye effluents. In the present study, we have used acid activated clay for adsorption of Basic Violet 2 dye from aqueous solution.

II. Experimental

2.1 Basic Violet 2 (Adsorbate): Basic Violet 2 (BV2) dye was chosen as adsorbate for the present work. It was procured from dye manufacturing company in Indore, M.P., India. It is a cationic dye having triarylmethane structure as backbone (Figure 1). Properties of BV2 are given in Table 1. Stock solution of dye (10^{-3} M) was prepared by dissolving accurately weighed dye into distilled water. Experimental solutions were freshly prepared by successive dilution of stock solution. Calibration curve (Figure 2) as a function of dye concentration was obtained using UV-Visible spectrophotometer (Systronics, Type 118).

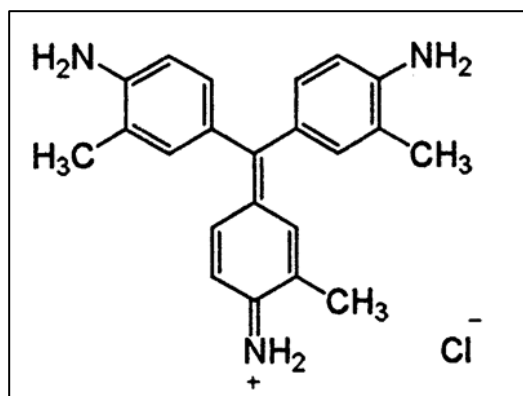


Figure 1: Chemical structure of BV2

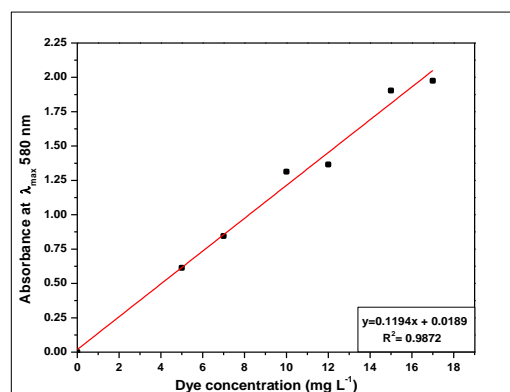


Figure 2: Calibration curve for different concentrations of dye at λ_{\max} 580 nm.

Table 1: Properties of BV2 dye.

C.I. No.	C.I.42520
CAS No.	3248-91-7
Other names	New Fuchsin
Molecular Formula	$C_{22}H_{24}ClN_3$
Molecular Weight (g/mol)	365.9
λ_{\max}	580 nm

2.2 Acid Activated Clay (Adsorbent) and its Characterization: Acid activated clay (AAC) was purchased from local firm of Indore, M.P., India. Chemical composition of AAC was determined using JEOL JSM 5600 Energy Dispersive X-ray spectrometer (EDX) attached with Scanning Electron Microscope (SEM). Powder X-ray diffractograms were recorded with Rigaku Diffractometer with CuK_{α} (λ 1.54Å) radiation in a 2θ range of 1° - 65° . The BET surface area and pore-size determination was done using volumetric gas adsorption method with advanced free space measurement using N_2 , Ar, CO_2 and other non-corrosive gases. FTIR spectra and SEM micrographs were recorded to investigate modification in the structure of adsorbent before and after adsorption. FTIR spectra were taken by KBr pellet technique using Bruker Vertex 70 FTIR spectrometer in the range 4000 to 400 cm^{-1} . SEM was used to determine the surface morphology of samples under study.

2.3 Batch Kinetics Experiments: Batch experiments were conducted by adding definite amount of adsorbent to 50 ml aqueous solution of particular dye concentration taken in Erlenmeyer flask of 150 ml capacity. After definite time intervals, 15 ml solution was subjected to centrifugation (centrifuge type C852/4, rpm 3500) and solution was analyzed for residual concentration using UV-Visible spectrophotometer. To study the effect of various parameters, same procedure was followed by altering one parameter and keeping others constant.

Adsorption capacity (q_t) is defined as the amount of dye adsorbed per gram of adsorbent. It is expressed in mg g^{-1} . Equation (1) was used to calculate it.

$$q_t = \frac{(C_i - C_o) * V}{m} \quad (1)$$

% Removal of the system, was determined by equation (2) –

$$\% \text{ Removal} = \left(\frac{C_i - C_o}{C_i} \right) * 100 \quad (2)$$

Where initial and final concentration of dye (mg L^{-1}) at time t is expressed as C_i and C_o , respectively, m is the mass (g) of clay and V is the volume (L) of dye solution used.

2.4 Kinetic Models : In order to predict rate of removal of any pollutant from aqueous solution, adsorption kinetics is studied. This will be helpful in designing the sorption treatment plants[9]. The kinetic data was fitted in Linear form of pseudo first order (PFO)[10] and pseudo second order (PSO)[11] models as given in equation (3) and (4).

$$\log(q_e - q_t) = \log(q_e) - \frac{K_1}{2.303}t \tag{3}$$

$$\frac{t}{q_t} = \frac{1}{K_2 q_e^2} + \frac{1}{q_e}t \tag{4}$$

Where q_e and q_t are amount of dye adsorbed per gram of adsorbent (mg g^{-1}) at equilibrium and at time t respectively, K_1 and K_2 are the rate constants for PFO and PSO models, respectively. By plotting a graph between $\log(q_e - q_t)$ versus t for equation (3) and t/q_t versus t for equation (4), we calculated the value of constants from slope and intercept.

2.5 Validity of Kinetic Models: The experimental data was fitted in PFO and PSO kinetic models and tested for applicability by comparing the values of R^2 and normalized standard deviation (nsd). The nsd[12] was calculated by equation (5). Higher values of R^2 and low values of Δq (%) indicated good fit between experimental and calculated data.

$$\Delta q (\%) = 100 * \sqrt{\frac{\sum[(q_{e \text{ exp}} - q_{e \text{ cal}})/q_{e \text{ exp}}]^2}{n - 1}} \tag{5}$$

where n is the number of data points, $q_e, \text{ exp.}$ (mg g^{-1}) is the experimental values and $q_e, \text{ cal.}$ (mg g^{-1}) is the calculated values by both PFO and PSO models.

2.6 Adsorption Mechanism: The mechanism of adsorption of BV2 dye onto AAC was investigated using Intraparticle diffusion model and Boyd kinetic model.

2.6.1 Intraparticle Diffusion Model (IPD) : Weber and Morriss' IPD model[13] is given by equation (6).

$$q_t = K_{ip}\sqrt{t} + C \tag{6}$$

If the linear plot of adsorbate uptake q_t versus square root of time $t^{1/2}$, passes through origin, then intraparticle diffusion was the rate controlling step. But if linear plot does not pass through origin then mechanism other than intraparticle diffusion are involved. However, if multilinear plot are obtained, then two or more steps influence the adsorption process.

2.6.2 Boyd Kinetic Model: This model is very important in determining the rate limiting step in the adsorption process. Equation (7) was used to calculate B_t values at different time interval t [14].

$$B_t = -0.4977 - \ln(1 - F) \tag{7}$$

where F is the fractional attainment of equilibrium at different time t and B_t is the function of F . Linearity of plot B_t versus t was used to distinguish between particle diffusion and film diffusion.

III. Results And Discussion

3.1 Characterization of AAC: Chemical composition of AAC (Table 2) was determined using EDX spectrum. From Table 2, it is clear that AAC mainly consist of SiO_2 and Al_2O_3 . AAC was further characterized for mineralogical composition, specific surface area and porosity. Figure 3 represents the XRD pattern of AAC showing basal spacing d (calculated by Bragg's Equation) for each peak and corresponding mineral. It is evident that montmorillonite clay was present as the major mineral in AAC, but some modification in the structure of the clay has occurred due to acid attack. However, other minerals like kaolinite, quartz and hematite were also present. The BET specific surface area and total pore volume for AAC as obtained by volumetric gas adsorption method was found to be $297 \text{ m}^2 \text{ g}^{-1}$ and $0.3779 \text{ cm}^3 \text{ g}^{-1}$, respectively. The high specific area makes AAC comparable with other natural materials used as adsorbent. The average pore diameter was 5.09 nm, which confirms that the adsorbent is mesoporous in nature[15].

Table 2: Chemical composition of Acid activated clay

Components	SiO_2	Al_2O_3	Fe_2O_3	CaO	TiO_2	SO_3	Cl	LOI ^a
% (by weight)	59.83	9.77	8.48	2.59	1.83	2.90	0.58	14.02

^aloss on ignition

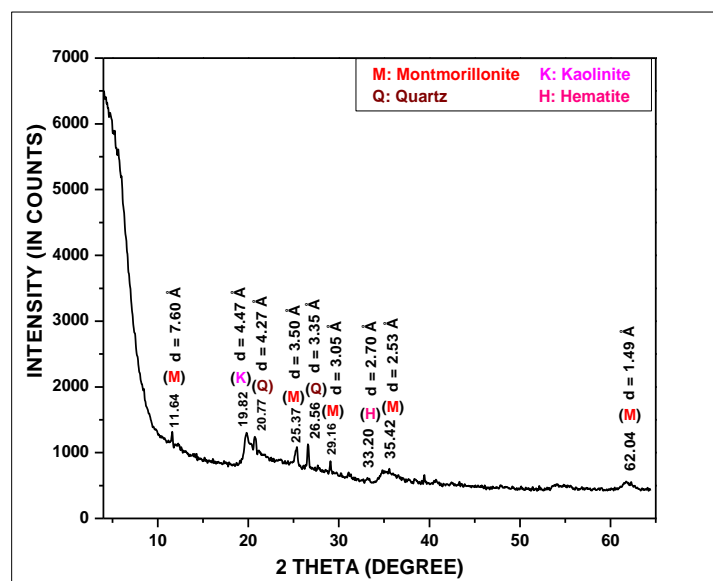


Figure 3: XRD pattern of AAC

3.2 FTIR and SEM studies before and after adsorption: Adsorption is a surface phenomenon. So during adsorption, change in surface morphology occurs which can be very easily studied with help of techniques like FTIR and SEM. FTIR is sensitive towards even little changes that occurs during adsorption. SEM gives information regarding the texture of the sample. So analysis has been done using both the techniques.

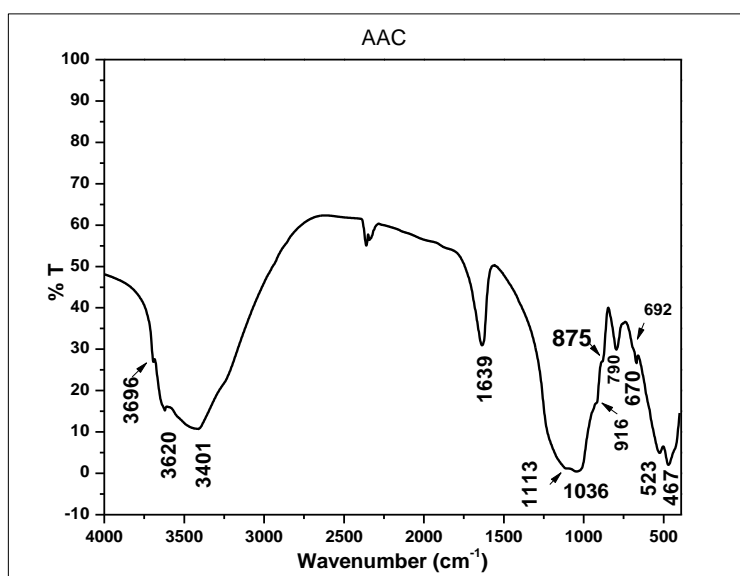


Figure 4: FTIR spectra of AAC before adsorption.

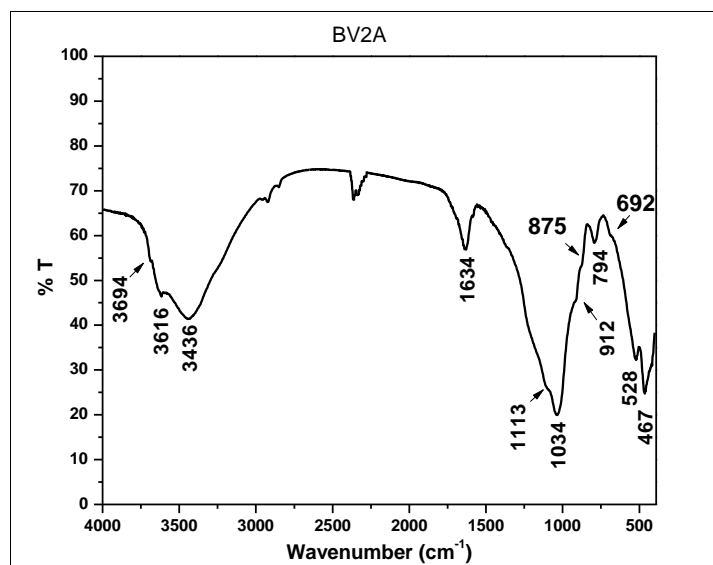


Figure 5: FTIR spectra of AAC after adsorption of BV2.

Figure 4 and 5 shows FTIR spectra of AAC before and after adsorption of BV2 dye. When the two spectra are compared, it was observed that change in position of bands (3696 cm^{-1} , 3620 cm^{-1} , 3401 cm^{-1} , 1639 cm^{-1} , 1036 cm^{-1} , 916 cm^{-1} , 790 cm^{-1} and 523 cm^{-1}) has occurred may due interaction between surface groups of adsorbent and dye molecule. This was indicative that adsorption has occurred. Further this was confirmed by SEM results shown in Figure 6.

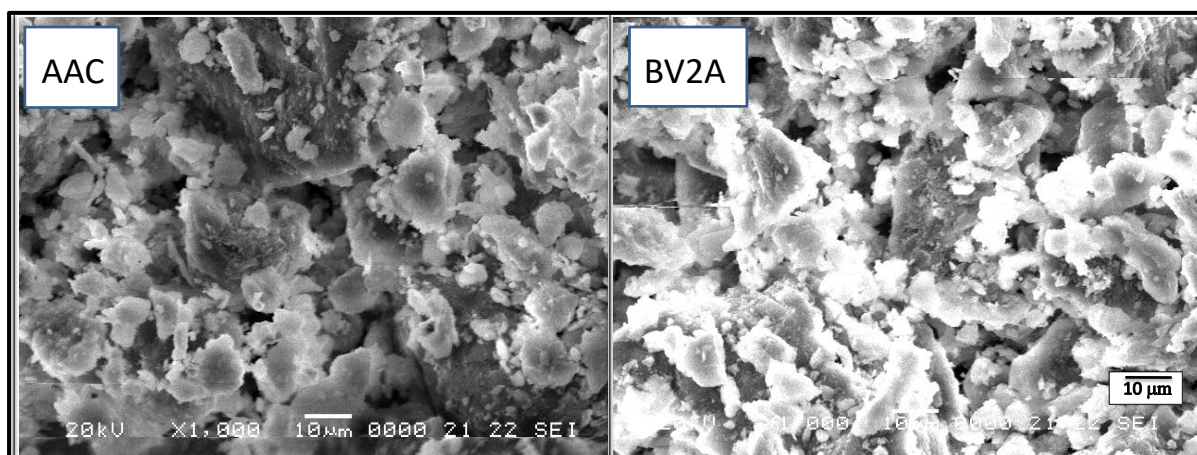


Figure 6: SEM images of acid activated clay (AAC) and dye adsorbed acid activated clay (BV2A).

The left panel of the Figure 6 shows the presence of pores on the surface of the adsorbent. These pores gets filled to maximum extent and adsorbent surface becomes saturated after adsorption (right panel of Figure 6). Thus change in texture of AAC has occurred due to adsorption.

3.3 Variation of Different Operating Parameters

3.3.1 Variation of contact time: Study of contact time is important to know the practical application of adsorption process. Figure 7 shows increase in removal of dye at various time intervals. Maximum dye was removed in first 10 minutes and the process almost becomes constant after this. It was observed that equilibrium was achieved in 30 minute for 10 mg L^{-1} of dye concentration. Initially adsorption sites were empty and were easily available for adsorption, therefore adsorption process was fast. Now when equilibrium was reached, some repulsion might have occurred between dye molecules adsorbed in the solid phase and those in present in solution, thus making unoccupied sites difficult to occupy. So adsorption becomes almost steady at this point [16] [17] Time required to reach the equilibrium was 30 minutes, so we chose 90 minutes contact time for further studies to ensure adsorption equilibrium.

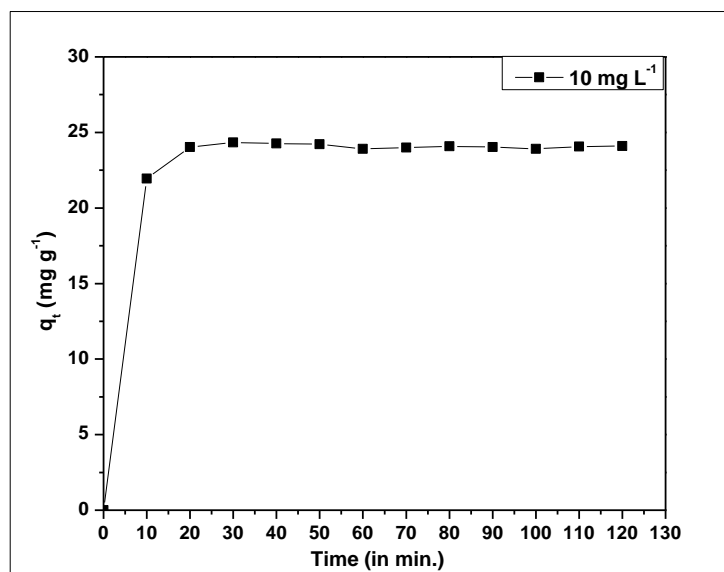


Figure 7: Variation of contact time (Conditions: Dye concentration = 10 mg L⁻¹, volume of dye solution = 50 ml, temperature=30 °C, mass of adsorbent = 0.02 gm, natural pH = 7.3)

3.3.2 Variation of Initial Concentration of Dye: Variation of initial dye concentration is an important parameter as removal of dye from solution is affected by it. From Figure 8 it was evident that as the dye concentration increased from 5 mg L⁻¹ to 17 mg L⁻¹, adsorption capacity also increased from 10.82 mg g⁻¹ to 39.31 mg g⁻¹. Also % removal increased from 79.77 % to 98.14 % (Figure not shown for brevity). This can be explained by the fact that as concentration of dye increases, driving force for the concentration gradient also increases [18].

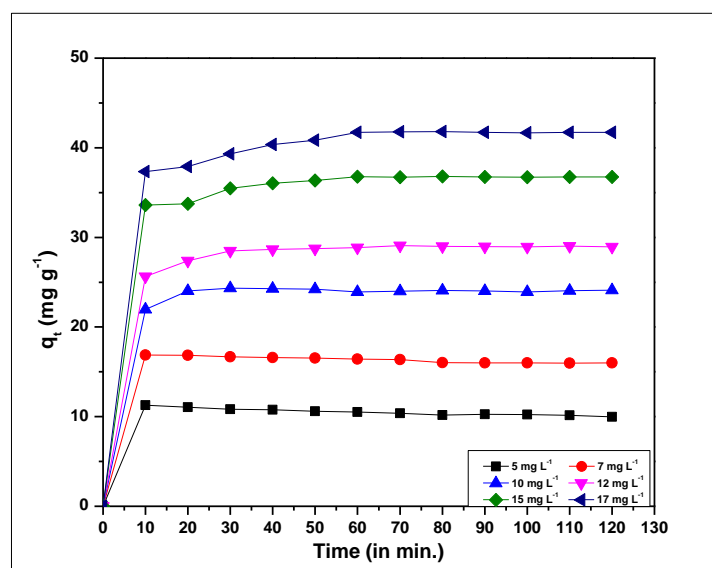


Figure 8: Variation of initial dye concentration. (Conditions: Volume of dye solution = 50 ml, temperature=30 °C, mass of adsorbent = 0.02 gm, natural pH = 7.3, contact time = 120 min.)

3.3.3 Variation of Mass of Adsorbent: The amount of adsorbent varied from 0.01-0.25 gm to study its effect on adsorption. Figure 9 depicts that removal of dye gradually increases by raising the adsorbent dose there by enhancing the adsorption process as more vacant sites were available for the phenomenon to take place[19]. When we consider amount of dye adsorbed per gram of adsorbent, adsorption capacity decreases steadily with the increasing amount of adsorbent. This may due to aggregation or overlapping of surface sites on adsorbent there by reducing the total surface area available for adsorption and increasing diffusion path length. [17],[16],[20]. Thus explains decrease in q_t from 47.80 mg g⁻¹ to 9.71 mg g⁻¹ with increasing mass of adsorbent from 0.01 to 0.025 gm. It was observed that after 0.05 gm of adsorbent dose, adsorption capacity almost becomes constant. Therefore, 0.05 gm is the best dosage for adsorption. But for convenience of study, we conducted our experiments by taking 0.02 gm of adsorbent.

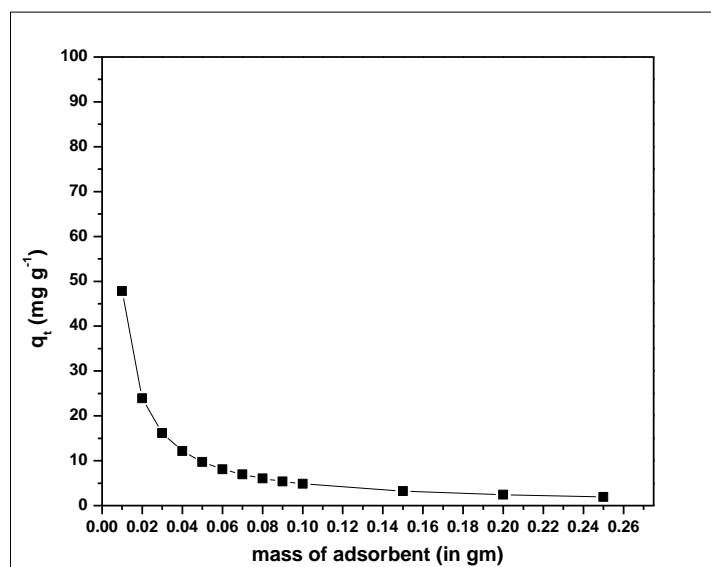


Figure 9: Variation of mass of adsorbent (Conditions: Dye concentration = 10 mg L⁻¹, volume of dye solution = 50 ml, temperature=30 °C, contact time = 90 min., natural pH = 7.3)

3.3.4 Variation of pH: pH is critical parameter affecting rate of dye uptake from solution. Variation of pH leads to degree of ionization of dye in aqueous solution and dissociation of surface active groups of adsorbent, thus affects adsorption process [21]. The pH was varied between 1 to 12. At low pH, minor variations were observed in adsorption capacity. As pH become acidic to alkaline there was increase in adsorption capacity. Again it becomes almost constant in alkaline pH (Figure 10). Less adsorption at low pH can be explained by competition occurring between cations of dye and protons for the negative adsorption sites on adsorbent surface. Now in alkaline pH, deprotonation of hydroxyl groups of clay makes the surface negatively charged. Thus increasing the adsorption process due to weak electrostatic force of attraction between both the species [22], [23].

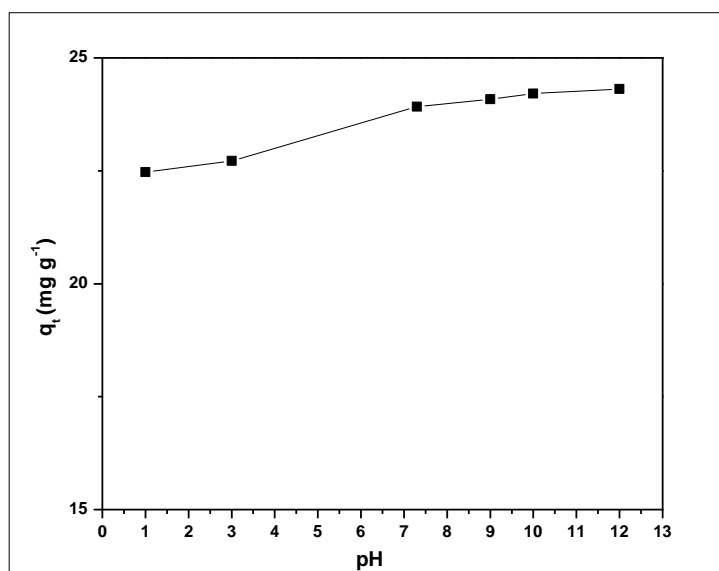


Figure 10: Variation of pH (Conditions: Dye concentration = 10 mg L⁻¹, volume of dye solution = 50 ml, temperature=30 °C, mass of adsorbent = 0.02 gm, contact time = 90 min.)

3.4 Kinetic Models: The kinetics of adsorption of BV2 onto AAC was investigated using PFO and PSO models shown in Figure 11 and 12, respectively. Kinetic constants calculated for both the models are given in Table 3. It was observed that for PFO model, the values of experimental q_e were not in agreement with calculated q_e . Also low values of average R_1^2 (0.8248) and high $\Delta q(\%)$ (20.9225) showed that the adsorption kinetics does not comply with PFO model. Now for PSO model, it is noteworthy to mention that with the increasing initial dye concentration (10 mg L⁻¹ to 17 mg L⁻¹), the calculated q_e are also increasing (15.87 to 42.25 mg g⁻¹) and is in

good agreement with experimental q_e values. The higher value of average R_2^2 (0.9998) and lower value of $\Delta q(\%)$ (1.13) clearly indicates that PSO model is better fitted in the experimental data than PFO.

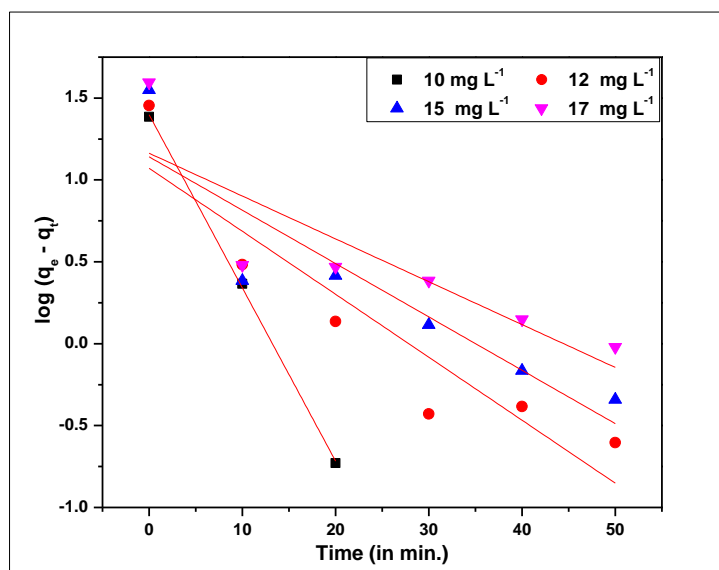


Figure 11: PFO kinetic plot for adsorption of BV2 onto AAC

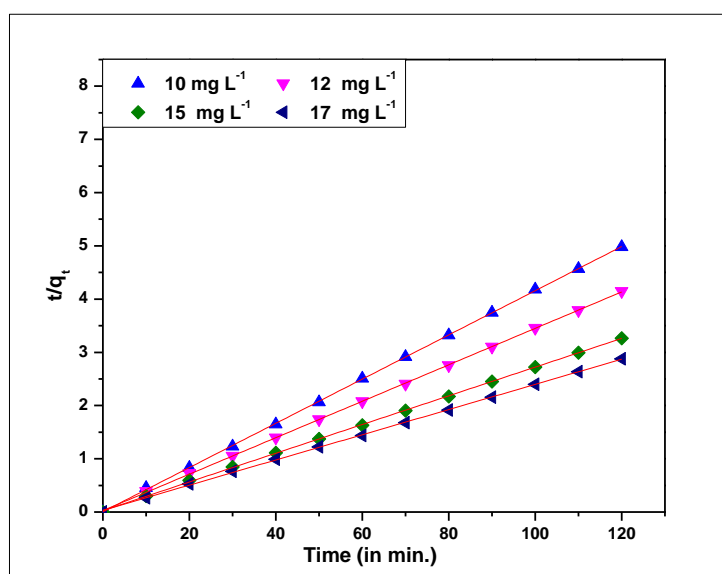


Figure 12: PSO kinetic plot for adsorption of BV2 onto AAC

Table 3: Values of regression coefficient (R_1^2 & R_2^2), $\Delta q(\%)$, PFO and PSO rate constant (K_1 & K_2), calculated and experimental q_e obtained at different initial concentration of BV2.

Kinetic model	Parameters	Concentration of BV2 aqueous solution (mg L^{-1})			
		10	12	15	17
Pseudo-first-order equation	$q_e, \text{exp. (mg g}^{-1}\text{)}$	24.33	28.49	35.47	39.31
	$K_1 (\text{min}^{-1})$	0.2436	0.0886	0.0751	0.0603
	$q_e, \text{cal (mg g}^{-1}\text{)}$	25.03	11.77	13.84	14.56
	R_1^2	0.9992	0.8313	0.7869	0.6818
	$\Delta q(\%)$	2.02	26.24	27.27	28.16
Pseudo-second-order equation	$K_2 (\text{g mg}^{-1} \text{min}^{-1})$	0.00512	0.02589	0.02584	0.03172
	$q_e, \text{cal (mg g}^{-1}\text{)}$	24.08	29.20	37.09	42.25
	$h (\text{mg g}^{-1} \text{min}^{-1})$	2.97	22.07	35.55	56.62
	R_2^2	0.9999	0.9999	0.9998	0.9997
	$\Delta q(\%)$	0.30	0.72	1.32	2.16

3.5 Adsorption Mechanism: The IPD and Boyd kinetic models were used in the study to predict the mechanism of adsorption of BV2 dye onto AAC. Figure 13 shows the IPD plot of BV2 dye adsorption onto AAC at various initial dye concentration at 30 °C with multi-linearity. Multi-linear plots represents different stages of adsorption mechanism. The first stage in the mechanism is external surface adsorption, second is intraparticle diffusion which is the rate-limiting step, and third is the final equilibrium which is very fast[24]. Multi-linear plots for adsorption of BV2 onto AAC suggests that intraparticle diffusion was not the rate limiting step for this material. The first initial portion of plot indicated an external mass transfer and intraparticle or pore diffusion whereas the second linear portion was due to the final equilibrium[24].

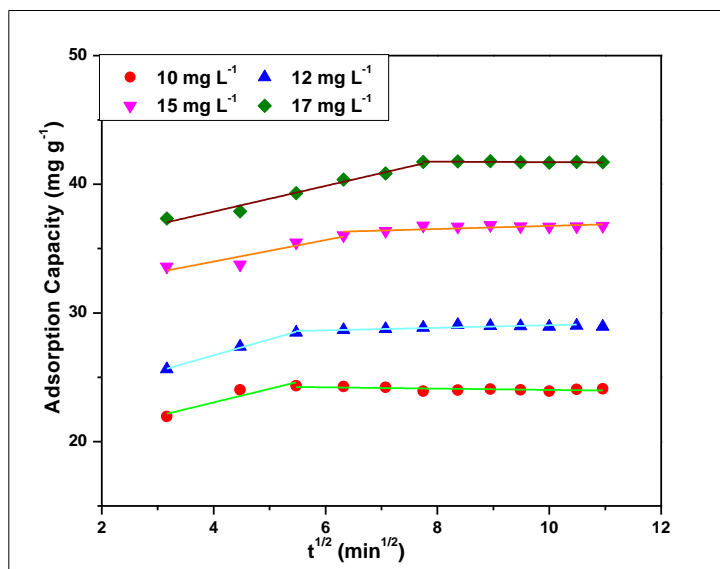


Figure 13: IPD plot for adsorption of BV2 onto AAC

Table 4: The values IPD rate constants K_{ip} , intercepts C and regression coefficients R_{ip}^2 .

		Concentration of BV2 aqueous solution (mg L ⁻¹)			
		10	12	15	17
Intraparticle diffusion	K_{ip1} (mg g ⁻¹ min ^{1/2})	1.05582	1.23967	0.83582	0.9979
	K_{ip2} (mg g ⁻¹ min ^{1/2})	-0.0501	0.10007	0.12118	-0.0179
	C_1 (mg g ⁻¹ min ^{1/2})	18.8223	21.7489	30.6505	33.8838
	C_2 (mg g ⁻¹ min ^{1/2})	24.5188	28.0453	35.5536	41.8988
	R_{ip1}^2	0.79308	0.99346	0.80788	0.9708
	R_{ip2}^2	0.34968	0.72141	0.47461	0.09639

The values of IPD rate constant K_{ip} and C obtained from the slope and intercepts of the IPD plot are shown in Table 4. The non-zero intercepts C at all stages suggest rate limiting step to be other than IPD in the adsorption process (Table 4). Moreover, the values of intercept C increase from first to last stage and also with increase in initial concentration, this may be due to boundary layer effect. The larger the intercept, the greater the contribution of the surface sorption in the rate controlling step[23].

Further the rate limiting step in the adsorption process was determined using Boyd kinetic model. Figure 14 shows Boyd plot for adsorption of BV2 dye onto AAC at different initial dye concentration at 30°C. This model helps in distinguishing between particle diffusion from surface diffusion of adsorbate molecules. In order to predict Boyd kinetic mechanism, the plot of B_t versus t should be tested for linearity. It was observed that for 10 mg L⁻¹ dye concentration, the plot was linear but does not pass through origin (Figure 14). Moreover, for higher initial concentrations of dye, plots were non-linear as well as does not pass through origin, thus it was concluded that adsorption of BV2 dye from its aqueous solution onto AAC adsorbent was governed by surface diffusion[25].

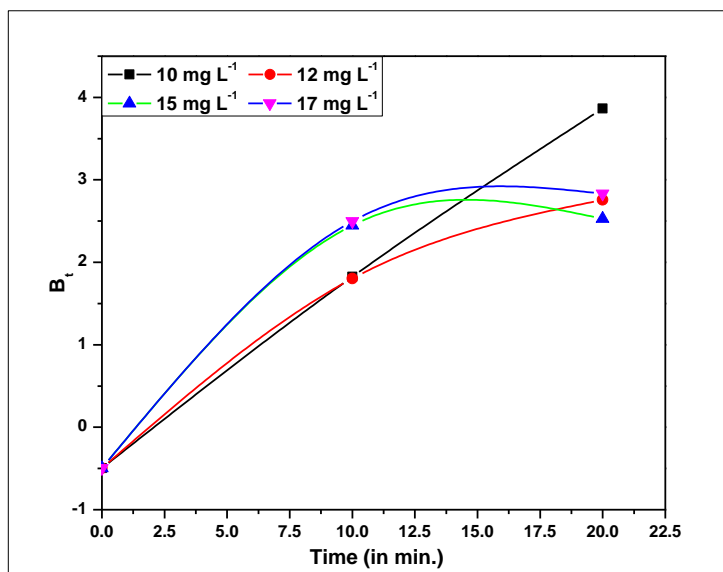


Figure 14: Boyd plot for adsorption of BV2 onto AAC

IV. Conclusion

For the sustainable remediation of water polluted by dyes, clay minerals and their modified forms are good alternative. Since natural form of clay has less ability for adsorption, we have used acid treated clay which proved to be an efficient adsorbent for the desired purpose. The adsorbent was characterized for its chemical composition, mineralogical composition and textural characteristics. It was found that AAC is mesoporous in nature with BET specific surface area $297 \text{ m}^2 \text{ g}^{-1}$ and total pore volume $0.3779 \text{ cm}^3 \text{ g}^{-1}$. XRD confirms the presence of montmorillonite as the major mineral with modified structure due to acid treatment. Shifting in the positions of FTIR spectra shows adsorption of BV2 onto AAC has occurred. SEM studies also confirms adsorption of dye onto AAC which was evident by observing surface of adsorbent getting saturated. Knowledge of both maximum adsorption capacity and mechanism of process is important. So focus on the factors influencing adsorption as well as kinetic models were done to completely understand the behavior of BV2 dye in contact with acid activated clay. It was found that the maximum removal of 98.14 % was achieved. Best adsorbent dose was 0.05 gm of AAC and alkaline pH was favorable for adsorption. Equilibrium was attained in 60 minutes. Further kinetic models were also applied with PSO model as better fitted model than PFO. Adsorption mechanism was predicted to be governed by surface diffusion as the rate controlling step. Thus from the above study it is concluded that natural materials like clay and their modified forms like acid activated clay are sustainable for dye removal from waste water.

Acknowledgement

Authors acknowledge UGC-DAE Consortium for Scientific Research, Indore for carrying out our FTIR, XRD and SEM-EDX measurements.

References

- [1] T. Kobayashi, *Applied environmental materials science for sustainability*. Chapter-1, IGI Global (2017). DOI: 10.4018/978-1-5225-1971-3.ch001
- [2] E. I. Unuabonah, C. Gunter, J. Weber, S. Lubahn, and A. Taubert, "Hybrid clay: A new highly efficient adsorbent for water treatment," *ACS Sustain. Chem. Eng.*, vol. 1, no. 8, pp. 966–973, 2013.
- [3] Y. T. Hung, S.T. Ong and P.S. Keng, "Low Cost Adsorbents for Sustainable Dye Containing-Wastewater Treatment," *Asian J. Chem.*, vol. 26, no. 7, pp. 1873–1881, 2014.
- [4] C. Su and Y. Wang, "Influence Factors and Kinetics on Crystal Violet Degradation by Fenton and Optimization Parameters using Response Surface Methodology," in *International Conference on Environmental and Agriculture Engineering*, vol. 15, pp. 76–80, 2011.
- [5] S. Nandhini, R., Vaishnavi V. Koti, Vadanandari, V. and Rangabhashiyam, "Decolorization studies of synthetic textile dye using Aspergillus species under static and shaking conditions," *Asian J. Sci. Technol.*, vol. 4, no. 11, pp. 10–12, 2012.
- [6] Z. S. Ashtouky, "Removal of indigo carmine dye from synthetic wastewater by electrochemical oxidation in a new cell with horizontally oriented electrodes," *Int. J. Electrochem. Sci.*, vol. 8, no. 1, pp. 846–858, 2013.
- [7] M. R. Samarghandi, M. Zarrabi, M. N. Sepehr, A. Amrane, G. H. Safari, and S. Bashiri, "Application of acidic treated pumice as an adsorbent for the removal of azo dye from aqueous solutions: kinetic, equilibrium and thermodynamic studies," *Iranian J. Environ. Health Sci. Eng.*, vol. 9, pp. 1–10, 2012.
- [8] F. Kooli, Y. Z. Khimiyak, S. F. Alshahateet, and F. Chen, "Effect of the acid activation levels of montmorillonite clay on the cetyltrimethylammonium cations adsorption," *Langmuir*, vol. 21, no. 19, pp. 8717–8723, 2005.

- [9] and Y.-C. H. Yuh-Shan Ho, Chun-Chiao Chiang, "SORPTION KINETICS FOR DYE REMOVAL FROM AQUEOUS SOLUTION USING ACTIVATED CLAY," *Sep. Sci. Technol.*, vol. 36, no. 11, pp. 2473–2488, 2001.
- [10] Y. S. Ho, "Citation review of Lagergren kinetic rate equation on adsorption reactions," *Scientometrics*, vol. 59, no. 1, pp. 171–177, 2004.
- [11] Y. S. Ho and G. McKay, "Pseudo-second order model for sorption processes," *Process Biochem.*, vol. 34, pp. 451–465, 1999.
- [12] B. Kayranli, "Adsorption of textile dyes onto iron based waterworks sludge from aqueous solution; isotherm, kinetic and thermodynamic study," *Chem. Eng. J.*, vol. 173, no. 3, pp. 782–791, 2011.
- [13] G. Vijayakumar, R. Tamilarasan, and M. Dharmendrakumar, "Adsorption, kinetic, equilibrium and thermodynamic studies on the removal of basic dye Rhodamine-B from aqueous solution by the use of natural adsorbent perlite," *J. Mater. Environ. Sci.*, vol. 3, no. 1, pp. 157–170, 2012.
- [14] P. Senthil Kumar, "Adsorption of Lead(II) Ions from Simulated Wastewater Using Natural Waste: A Kinetic, Thermodynamic and Equilibrium Study," *Environ. Prog. Sustain. Energy*, vol. 33, no. 1, pp. 55–64, 2014.
- [15] Y. S. Al-Degs, M. I. El-Barghouthi, A. H. El-Sheikh, and G. M. Walker, "Effect of solution pH, ionic strength, and temperature on adsorption behavior of reactive dyes on activated carbon," *Dye. Pigment.*, pp. 1–8, 2007.
- [16] S. Khorramfar, N. M. Mahmoodi, M. Arami, and K. Gharanjig, "Equilibrium and kinetic studies of the cationic dye removal capability of a novel biosorbent *Tamarindus indica* from textile wastewater," *Color. Technol.*, vol. 126, no. 5, pp. 261–268, 2010.
- [17] M. Sadeghi-Kiakhani, M. Arami, and K. Gharanjig, "Preparation of chitosan-ethyl acrylate as a biopolymer adsorbent for basic dyes removal from colored solutions," *J. Environ. Chem. Eng.*, vol. 1, no. 3, pp. 406–415, 2013.
- [18] O. Gulnaz, A. Kaya, F. Matyar, and B. Arikan, "Sorption of basic dyes from aqueous solution by activated sludge," *J. Hazard. Mater.*, vol. 108, no. 3, pp. 183–188, 2004.
- [19] F. Kooli, Y. Liu, R. Al-Faze, and A. Al Suhaimi, "Effect of acid activation of Saudi local clay mineral on removal properties of basic blue 41 from an aqueous solution," *Appl. Clay Sci.*, vol. 116–117, pp. 23–30, 2015.
- [20] L. Jayalakshmi, V. Devadoss, K. Ananthakumar, and G. Kanthimathi, "Adsorption Efficiency of Natural Clay towards the Removal of Naphthol Green Dye from the Aqueous Solution : Equilibrium and Kinetic Studies," *Int. Res. J. Environ. Sci.*, vol. 3, no. 5, pp. 21–26, 2014.
- [21] P. Pimol, K. Meevasana, and P. Prasert, "Influence of particle size and salinity on adsorption of basic dyes by agricultural waste: dried Seagrass (*Caulerpa lentillifera*)," *J. Environ. Sci.*, vol. 20, pp. 760–768, 2008.
- [22] B. Karima, B. L. Mossab, and M. A-hassen, "Removal of Methylene Blue from aqueous solutions using an Acid Activated Algerian Bentonite : Equilibrium and Kinetic Studies," *Int. Renew. Energy Congr.*, pp. 360–367, 2010.
- [23] B. H. Hameed, D. K. Mahmoud, and A. L. Ahmad, "Equilibrium modeling and kinetic studies on the adsorption of basic dye by a low-cost adsorbent: Coconut (*Cocos nucifera*) bunch waste," *J. Hazard. Mater.*, vol. 158, no. 1, pp. 65–72, 2008.
- [24] L. guo Yan, X. quan Shan, B. Wen, and G. Owens, "Adsorption of cadmium onto Al13-pillared acid-activated montmorillonite," *J. Hazard. Mater.*, vol. 156, no. 1–3, pp. 499–508, 2008.
- [25] A. S. Sartape, A. M. Mandhare, V. V. Jadhav, P. D. Raut, M. A. Anuse, and S. S. Kolekar, "Removal of malachite green dye from aqueous solution with adsorption technique using *Limonia acidissima* (wood apple) shell as low cost adsorbent," *Arab. J. Chem.*, pp. 1–10, 2014.

International Journal of Engineering Science Invention (IJESI) is UGC approved Journal with Sl. No. 3822, Journal no. 43302.

Soniya Sharma. "Use of Natural Material – Clay for Sustainable Treatment of Water Polluted By Dyes." International Journal of Engineering Science Invention (IJESI) , vol. 6, no. 9, 2017, pp. 71–81.